Optimum threshold setting for a positron-sensitive probe with background rejection capability

Seiichi Yамамото,* Kenichi Matsumoto** and Michio Senda**

*Department of Electrical Engineering, Kobe City College of Technology
**Department of Image Based Medicine, Institute of Biomedical Research and Innovation

In a positron-sensitive probe composed of a plastic scintillator and a bismuth germanate (BGO), scattered annihilation photons in the plastic scintillator become background counts. Although these scattered annihilation photons can be rejected by higher threshold level settings for the scintillation pulse of the plastic scintillator and for that of the BGO, the system sensitivity is reduced. We have theoretically and experimentally optimized the threshold levels for both the plastic scintillator and the BGO. After calculating the energy loss in the plastic scintillator and the BGO for the scattered annihilation photons, we measured the background counts of a positron-sensitive probe by changing these threshold levels. Results revealed that one optimum threshold setting of the positron-sensitive probe was 0.3 of the peak level of the pulse for the plastic scintillator and 0.7 of that for the BGO. With these threshold levels, the background counts could be decreased to less than 0.2% of the true positron counts.

Key word: positron, probe, background, threshold

INTRODUCTION

INTRA-OPERATIVE PROBES have recently become important instruments in nuclear medicine for use in radio-guided surgery.[1,2] The radiopharmaceutical F-18-fluorodeoxy-glucose (FDG) shows promise in this application for tumor detection[1,3–5] while several methods have been proposed for positron-sensitive probes in intra-operative use.[6–8] A problem associated with these positron sensitive probes has been the relatively high background counts due to the presence of 511 keV annihilation photons. In the case of beta probes, annihilation photons could also be detected, and the separation of beta particles (positrons) from annihilation photon has been difficult because the maximum energy of F-18 (632 keV) is close to 511 keV. In the case of detection of annihilation photons, they penetrated the gamma shield in large quantities and background radiation counts increased.

One promising method for minimizing the background counts is to use a phoswich positron-sensitive probe.[9,10] This method employs two stacked scintillators with different decay times. The first scintillator detects positrons and the second detects annihilation photons. If these two events occur simultaneously, the event is a true positron detection event because positron detection is followed by the detection of gamma photons. If only one of these events occurs, the event is rejected as an annihilation photon event. This configuration has been applied to a continuous blood sampling system by the authors.[11] One problem with this positron-sensitive probe is the presence of scatter events in the first scintillator. Some of these events can be recognized as true events because both the first scintillator and second scintillator can produce scintillation photons simultaneously if the scattered events are detected by the BGO. However, although these scattered annihilation photons can be rejected by higher threshold level settings for scintillation pulses of the first and second scintillators, the sensitivity of the system decreases. Consequently, we have optimized the threshold levels for the first and second scintillators theoretically and experimentally to minimize the background counts while maintaining higher system sensitivity.

MATERIALS AND METHODS

Description of the positron-sensitive probe

Figure 1 shows a schematic diagram of the positron-sensitive probe used for optimizing the threshold setting. The probe consists of a plastic scintillator, a BGO, and a photo-multiplier tube (PMT). Here, a positron emitted from F-18 is detected by the plastic scintillator. The positron loses its energy in the plastic scintillator (optically coupled to the BGO) and emits two annihilation photons in opposite directions. Though one of the photons escapes from the detector, the other is directed to the BGO where it is detected. In this case, a fast scintillation pulse of the plastic scintillator and a slow scintillation pulse of the BGO can be observed. When the background annihilation photon is detected by the plastic scintillator, only the fast component is observed, and when the background annihilation photon is detected by the BGO, only the slow component is observed. By using the pulse shape information, these two types of background events can be rejected making it possible to selectively detect positrons with the probe.

Conceivably a scattered annihilation photon in the first scintillator could be recognized as a true event. We show the schematic diagram of the positron-sensitive probe showing the scattered annihilation photons interacted in the plastic scintillator in Figure 1 (B). In this case, the annihilation photon is scattered in the plastic scintillator, loses some of its energy (E1), and changes its direction to BGO. The scattered photon is detected by the BGO and loses its energy (E2). Because both the first scintillator and second scintillator could produce scintillation photons simultaneously, this scattered event might be recognized as a positron event if the threshold settings of the system are inadequate. The threshold settings also affect the sensitivity of the system, so it becomes important to optimize the threshold settings.

Figure 2 shows a photograph of the positron-sensitive probe used for the experiments for optimizing the threshold settings. The size of the plastic scintillator was 20 mm diameter and 2.5 mm thick. This plastic scintillator was optically coupled to a BGO 25 mm in diameter and 25 mm high, and the BGO was optically coupled to a 25 mm diameter round PMT (Hamamatsu R-1924). These parts were contained within a 4 mm thick tungsten shield. At the one end of the shield was placed a collimator with an 18 mm diameter and 5 mm deep hole. This large probe was not for intra-operative use but intended for some experiments including this study. The reason for the use of this larger probe is that it has an advantage of high sensitivity, so it is easier to confirm its pulse shapes for threshold settings. The design and performance of the intra-operative probe of smaller size employing this configuration will be presented in an other paper.

The PMT's output is fed to a delayed integration circuit to distinguish whether the event is a positron event or an
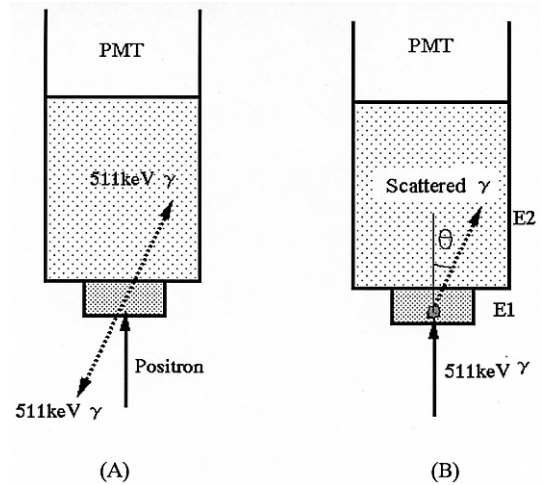

Fig. 1 Schematic diagram of the positron-sensitive probe for detecting positrons (A), and scattered annihilation photons (B).
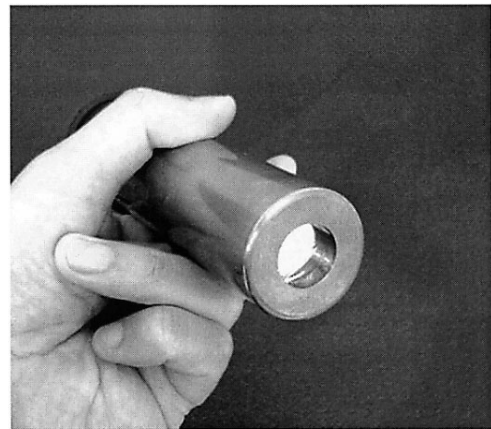

Fig. 2 Photograph of the large size positron-sensitive probe used in the experiments for optimizing the threshold settings.
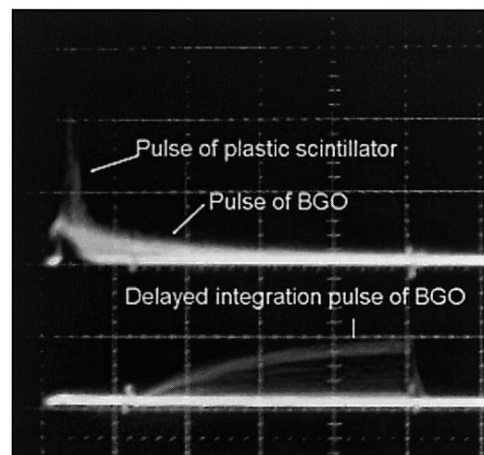

Fig. 3 Pulse shape of the input (*top*) and delayed integrated signal (*bottom*) of the positron-sensitive probe. The horizontal axis is 200 ns per division.

annihilation photon event.[11] In Figure 3, we show the pulse shapes of the input and delayed integrated signal of the positron-sensitive probe. The polarization of the integrated signal is inverted to more clearly show the pulse shape. The first threshold is set for the plastic scintillator's input pulse (fast component) and the second threshold is for the BGO's delayed integration signal. For reference data, we measured energy spectrum of the plastic scintillator for beta particles of similar energy and that of the BGO for 511-keV gamma photons.

Theoretical optimum threshold levels
When an annihilation photon of energy E is scattered in the plastic scintillator and is detected in the BGO, the following equation is derived,

$$E = E1 + E2 \qquad (1)$$

Where energy absorbed in the plastic scintillator is E1 and that in the BGO is E2.

Here, E2 is the function of the scattered angle θ described in Eq. (2);

$$E2 = E/(2 - \cos \theta) \qquad (2)$$

This equation is derived from the relation between energy of the scattered radiation (E2) and the scatter angle (θ) of the Compton scatter event when the incident gamma energy (E) is 511-keV.[12]

From Eq (1) and Eq (2), we obtain the following equation;

$$E1 = E - E2 = E(1 - \cos \theta)/(2 - \cos \theta) \qquad (3)$$

By plotting the Eq (2) and Eq (3), we can determine the energy absorption of the scattered annihilation photons in the plastic scintillator and BGO as a function of the scatter angle. If the threshold level for plastic scintillator is higher than E1 and the threshold level for BGO is higher than E2, then theoretically all of the scattered events can be rejected.

Experimental optimization of the threshold settings
First, the second threshold for the BGO pulse was fixed to 70% of the photo-peak level of the annihilation photon, then the first threshold level for the plastic scintillator was changed, and the positron and background count rates were measured. The threshold level of 70% was selected because of the relatively poor energy resolution of the BGO for the annihilation photons. An F-18 point source of around 1 MBq contained in a tungsten collimator was placed 5 mm from the probe surface. The background count rate was measured by inserting a 2 mm thick aluminum plate between the F-18 and the probe. It was done this way because the aluminum plate is so thick that the all the positrons from F-18 are absorbed while the annihilation photons can pass through the plate with very small interactions of less than 3%. Next, the first threshold was fixed to 30% of the peak for the plastic scintillator pulse,
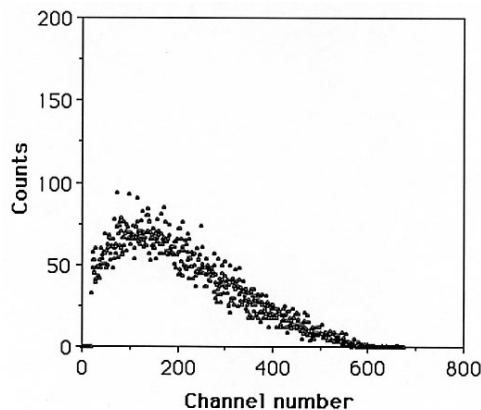
(A)
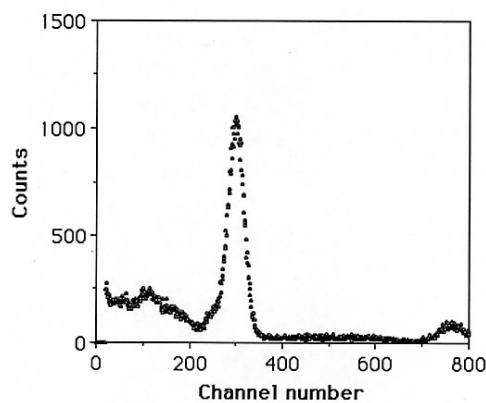
(B)

Fig. 4 Energy spectrum of plastic scintillator for Tl-204 beta particles (maximum energy 743-keV, similar to F-18-positron, 632-keV) (A) and that of BGO for Na-22 gamma photons (511-keV plus 1.27-MeV gamma) (B).

while the second threshold was changed and the positron and background count rates were measured. Positron and background count rates were measured by a rate meter for 30 sec and were converted to count per sec (cps) to reduce the statistical uncertainty. Decay correction for F-18 (110 min) was performed for the measured data.

RESULTS

Energy spectra of plastic scintillator and BGO
Figure 4 (A) shows the energy spectrum of the plastic scintillator for beta particles of Tl-204 (maximum energy 743-keV, similar to F-18-positron, 632-keV). Also we show the energy spectrum of BGO for 511-keV gamma photons of Na-22 (511-keV plus 1.27-MeV gamma) in Figure 4 (B). The amplifier gain for the energy spectrum of BGO was twice of that for the plastic scintillator. Energy resolution of BGO for 511-keV gamma photons was 13.3% full width at half maximum (FWHM). These data were not measured in the phoswich detector but were measured independently optically coupled to a PMT
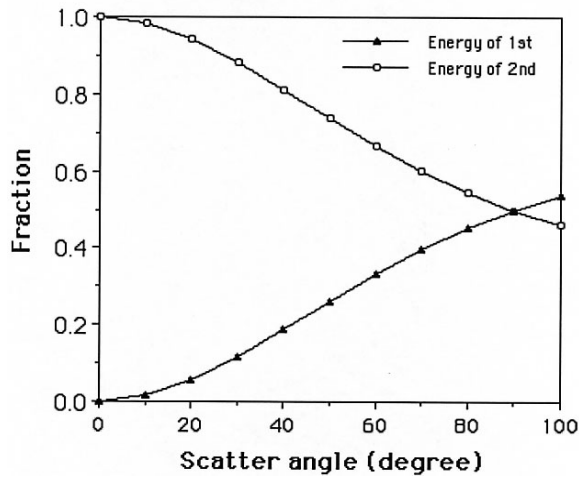
Fig. 5 Energy absorption of the scattered gamma photon in the first scintillator and the second scintillator as a function of scattered angle.
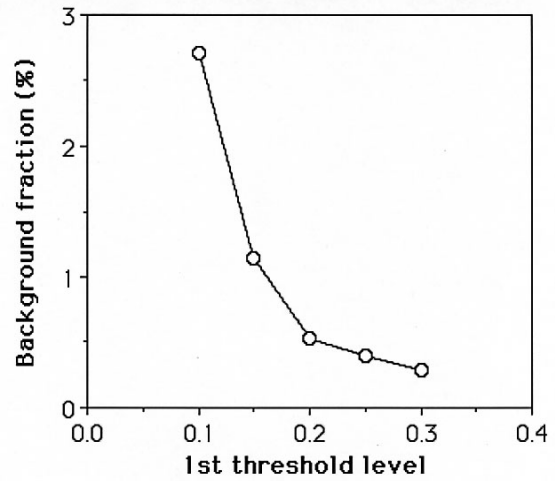

Fig. 7 Background fraction (background count rate/true count rate) as a function of the first threshold level at the second threshold level of 0.7.
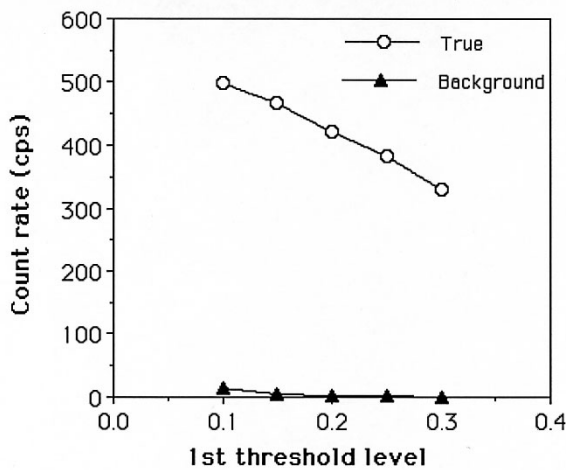

Fig. 6 Positron (true) count rate and background count rate as functions of the first threshold level at the second threshold level of 0.7.
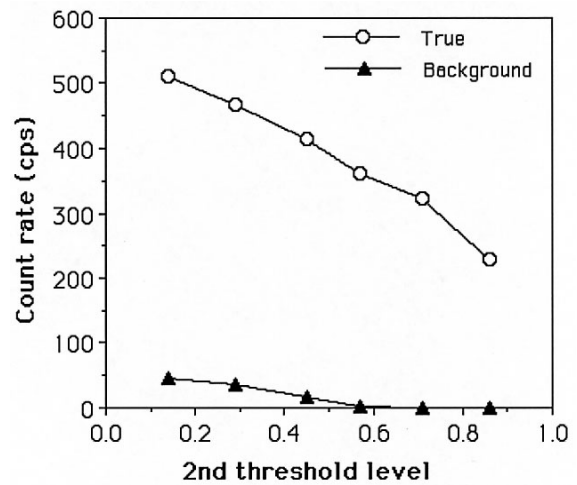

Fig. 8 Positron (true) count rate and background count rate as functions of the second threshold level at the first threshold level of 0.3.

because of the difficulty of the separation of these two signals in phoswich configuration. In addition, the energy spectrum of the BGO was not the delayed integration signal but the full integration signal. So the energy resolution shown here was better than in the phoswich configuration.

Theoretical optimum threshold levels
Figure 5 presents the energy absorption of the scattered annihilation photons in the plastic scintillator and BGO as a function of the scatter angle. If the threshold level for the plastic scintillator is higher than E1 and the threshold level for the BGO is higher than E2, all of the scattered events can theoretically be rejected. With this result, it became clear that with a higher first threshold, one can set

a lower level for the second threshold, and vice versa. For example, to reject the scatter annihilation photons with a scatter angle of 60 degree, the first threshold level needs to be set above 0.3 and the second threshold level needs to be set above 0.7 to reject all of the scattered events. Gamma photons scattered at smaller angles will be rejected by the first threshold, while those scattered at larger angles will be rejected by the second threshold.

Experimental optimization of the threshold settings
In Figure 6, we show the positron count rate and background count rate as functions of the first threshold at the second threshold level of 0.7. As the first threshold increased, both the positron count rate and the background count rate decreased. To optimize the signal-to-noise
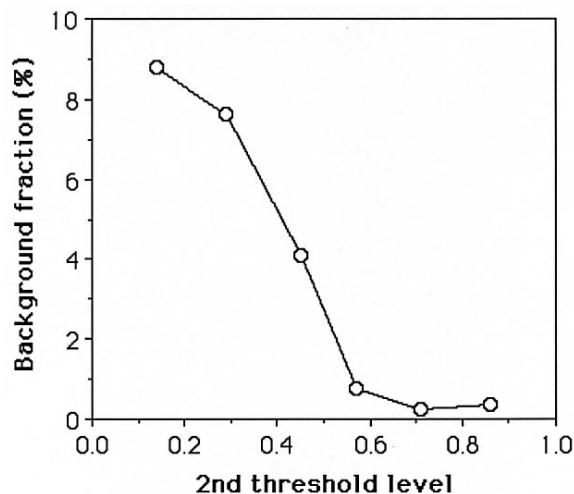
Fig. 9 Background fraction (background count rate/true count rate) as a function of the second threshold level at the first threshold level of 0.3.

ratio, we calculated the background noise fraction defined as a ratio of the background count rate to the positron (true) count rate. The background fraction as a function of the second threshold is shown in Figure 7. The background fraction decreased rapidly as the second threshold was increased from 0.1 to 0.2; above the first threshold of 0.2, the background fraction was less than 0.5%.

In Figure 8, we show the positron count rate and background count rate as functions of the second threshold at the first threshold level of 0.3. As the second threshold level increased both the positron count rate and the background count rate decreased.

The background fraction as a function of the first threshold is shown in Figure 9. The background fraction decreased rapidly as the second threshold increased from 0.14 to 0.57. Above the second threshold of 0.7, the background fraction was less than 0.5%. With these results, we determined one of the optimum first threshold levels as 0.3 and second threshold level as 0.7.

DISCUSSION AND CONCLUSION

We determined the optimum threshold levels for a positron-sensitive probe composed of a plastic scintillator and a BGO. Results indicate that the threshold levels were at least one of the optimum settings for the probe. There may also be other threshold levels for optimization. We found that when the first threshold setting is low, the second threshold level must be high to eliminate the scattered annihilation photons. For example, for a scattered angle of 20 degrees, the first threshold level could be lowered to less than 0.1 of the peak value. However, in that case, the second threshold level must be more than 0.9, which will decrease the sensitivity due to limiting energy resolution of the BGO for annihilation photons. In addition, since the integration of the BGO signal is a delayed one, the energy

resolution becomes worse than in the case of full integration; therefore, the first threshold level cannot be set too low. On the other hand, if one sets a higher first threshold level, the second threshold level can be lower. For example, if the scattered angle is 90 degrees, the first threshold level is 0.5 of the peak level, and thus the second threshold can be set to 0.5. In this case, some fractions of the positrons detected by the plastic scintillator are also rejected by the first threshold. With these considerations, the first threshold level of 0.3 and second threshold level of 0.7 are at least near optimization.

We believe the threshold setting discussed in this paper can be applied to other positron-sensitive probes using different scintillator combinations, because the energy absorptions in the scintillators are expressed in Eq (2) and Eq (3), and these equations are independent of the materials. In conclusion, if the energy resolution of the second scintillator is good, the second threshold can be set higher. When this happens, the first threshold can be set lower, and thus the system sensitivity is higher.

REFERENCES

1. Hoffman EJ, Tornai MP, Janecek M, Patt BE, Iwanczyk JS. Intraoperative probes and imaging probes. *Eur J Nucl Med* 1999; 26 (8): 913–935.
2. Britten AJ. A method to evaluate intra-operative gamma probes for sentinel lymph node localization. *Eur J Nucl Med* 1999; 26 (2): 76–83.
3. Essner R, Hsueh EC, Haigh PI, Glass EC, Huynh Y, Daghighian F. Application of an F-18-fluorodeoxyglucose-sensitive probe for the intraoperative detection of malignancy. *J Surg Res* 2001; 96: 120–126.
4. Zervos EE, Desai DC, Depalatis LR, Soble D, Martin EW. F-18-labeled fluorodeoxyglucose positron emission tomography-guided surgery for recurrent colorectal cancer: a feasibility study. *J Surg Res* 2001; 97: 9–13.
5. Desai DC, Arnold M, Saha S, Hinkle G, Soble D, Fry J, et al. Correlative whole-body FDG-PET and intraoperative gamma detection of FDG distribution in colorectal cancer. *Clinical Positron Imaging* 2000; 3 (5): 189–194.
6. Lederman RJ, Raylman RR, Fisher SJ, Kison PV, San H, Nabel EG, et al. Detection of atherosclerosis using a novel positron-sensitive probe and 18-fluorodeoxyglucose (FDG). *Nucl Med Commun* 2001; 22 (7): 747–753.
7. Daghighian F, Mazziotta JC, Hoffman EJ, Shenderov P, Eshaghian B, Siegel S, et al. Intraoperative beta probe: a device for detecting tissue labeled with positron or electron emitting isotopes during surgery. *Med Phys* 1994; 21 (1): 153–157.
8. Yasuda S, Makuuchi H, Fujii H, Nakasaki H, Mukai M, Sadahiro S, et al. Evaluation of a surgical gamma probe for detection of ^{18}F-FDG. *Tokai J Exp Clin Med* 2000; 25 (3): 93–99.
9. Levin CS, Tornai MP, MacDonald LR, et al. Annihilation gamma ray background characterization and rejection for a small beta camera used for tumor localization during surgery. *IEEE Trans Nucl Sci* 1997; 44: 1120–1126.
10. Tornai MP, Levin CS, MacDonald LR, et al. A miniature

phoswich detector for gamma-ray localization and beta imaging. *IEEE Trans Nucl Sci* 1998; 45: 1166–1173.

11. Yamamoto S, Tarutani K, Suga M, Minato K, Watabe H, Iida H. Development of a phoswich detector for a continu-ous blood sampling system. *IEEE Trans Nucl Sci* 2001; 48: 1408–1411.

12. Knoll GF. *Radiation detection and measurements, third edition*, John Wiley & Sons, Inc., 2000.